Influence of Increased Insulation Levels on Regional Air-Quality

Report by DMI and ECOFYS for EURIMA

Influence of Increased Insulation Levels on Regional Air-Quality

Energy savings and emission reduction by changing European building insulation standards in 2009

Ulrik Smith Korsholm, Bjarne Amstrup, Jens Havskov Sørensen, Shiyu Zhuang and Thomas Boermans

Danish Meteorological Institute, Research Department and ECOFYS

Acknowledgements

This study was sponsored by the European Insulation Manufactors Association (EURIMA) and the authors wish to thank EURIMA for access to previous reports and data. Measurements of ozone air concentrations was supplied by the Federal Environment Agency (Umweltbundesamt), Air Monitoring Network, Germany, the Latvian Environment, Geology and Meteorology Centre, LVGMC, the Hungarian Meteorological Service and the Swedish Environmental Research Institute (IVL).
The authors also wish to thank the European MEGAPOLI project for usage of the Base Year 2005 emission inventory. The research leading to creation of the "Base Year (2005) MEGAPOLI European Gridded Emission Inventory" has received funding from the European Union Seventh Framework Programme FP/2007-2011 within the project MEGAPOLI, grant agreement n212520.

Executive summary

This report presents the results of a project collaboration between the European Insolation Manufactorers Association (EURIMA), ECOFYS and the Danish Meteorological Institute (DMI). The aim has been to quantify the effect of increased insulation levels in Europe from 2009 to 2020. Emission reductions of criteria pollutants were estimated from projected energy savings as averages over European climate zones: cold (zone 1), moderate (zone 2), warm (zone 3), eastern European Union (EU) north (zone 4), eastern EU central (zone 5) and eastern EU south (zone 6). An air-quality model was used to simulate a status quo baseline scenario for 2009 and a corresponding reduced emission scenario. Annual, seasonal and monthly averages were considered, and the main findings include:

- Sulphur dioxide emissions decreased by 6.3 % and particulate matter by 9.0 % in zone 2 due to increased insulation levels. In zone 3 and 5 particulate matter emissions decreased by 5.3 % and 5.1 % respectively.
- Sulphur dioxide concentration in air near the surface decreased by 5.2 % to 6.2 % in zone 2 throughout the seasons. Great Britain, Belgium, the Netherlands and a part of northern France experienced seasonally average reductions of 6 % to 10 %. In Poland an average reduction of about 2 % was sustained throughout the seasons. Other countries experienced reductions between 0 % and 2 %.
- Total particulate matter concentrations in air near the surface decreased by 2.6 % to 3.6 % in zone 2. Germany, France, Belgium and the Netherlands had a sustained average reduction of about 3 % throughout the seasons, while it increased to 5 % over United Kingdom during spring. Countries outside zone 2 experience smaller reductions. Over Spain the reduction was about 2 % throughout the seasons.
- Ozone air concentrations near the surface increased by up to 3 % over major pre-curser sources during the winter season. A band of increased ozone extended from mid-England to Poland covering northern France, Belgium, the Netherlands, Germany and Poland. In other countries no significant changes were found. During the spring, summer and autumn only mid-England showed an increase (1 % to 2.5 %) while other countries remained neutral.

In future studies the effect of countries not included here such as Russia or Ukraine should be included in order to improve the long range effects of the emission reductions. Further investigations into the effects of different modes of meteorological variability on the conclusions presented here should also be carried out. For example the effect of the North Atlantic Oscillation or projected climate changes by 2020 could be incorporated. Further issues that have not been incorporated in the present study include the influence of the initiation of a cap and trade program for NO_x and SO_2 in Europe and the effect of projected emission changes due to increased emission control strategies both at the political, industrial and the technological level. Furthermore, the explicit effects of member state energy and heat planning and policies as well as their economical feasibility have not been considered.

Introduction

This report summarizes the outcome of a project collaboration between the the European Insulation Manufacturers Association (EURIMA), ECOFYS and the Danish Meteorological Institute (DMI). The main aim has been to quantify the effect of building insulation on regional air-quality levels in Europe. A similar study estimating the effect of building insulation on climate (specifically carbon dioxide emissions) has previously been conducted (SBi, 2009). The present project focuses on shorter lived tropospheric trace gases and should be viewed as auxiliary to previous studies. Advantages of increased building energy effeciency are normally expressed in terms of economic payback and includes lowering of energy bills for citizens and governments, reducing exposure to energy supply problems, minimizing stress on electricity supplies and generation of new green collar jobs. Within this project we attempt to go beyond the estimation of CO_2 emission savings and include European environmental benefits on shorter time scales into the framework.

The basic premise of the study is that increased levels of building insulation leads to a decrease in energy consumption whereby the national energy mix changes and emissions of air pollutants resulting from incomplete combustion declines. The project comprised three phases. In the first, energy reductions by 2020 due to increased insulation standards were estimated. In the second phase, the emission reductions were estimated and corresponding emission inventories were generated. In the last part, an air-quality model was used to quantify the effects of the emission changes on European air-quality levels. This report presents the main results of the project and discusses the possibilities for future work.

The main air pollutants in terms of health effects comprise ozone, particulate matter, sulphur-dioxide, nitrogen oxides and carbon monoxide. Ozone is a secondary specie which is generated via photochemical reactions with pre-curser gases such as volatile organic compounds and nitrogen oxides while the other gas-phase species are primary. Particulate matter has both a primary and a secondary component. The project focusses on these species and the quantification of the effect of increased insulation levels was done by comparing simulations with an air-quality model with baseline and reduced emissions. The baseline year was chosen as 2009 while 2020 was used as target year. From the air-quality modelling perspective, only emissions were assumed to change within the considered period thereby isolating the effect of insulation.

The base year, 2009, was dominated by warmer than average (with respect to the period 1971-2000) surface temperatures during summer months in Europe. August and September ranked as the second warmest (global average) ever recorded. Despite the warm summer in Europe ozone levels were low (EEA, 2010a). That year Europe experienced fewer exceedences of the information threshold ($180\,\mu g\,m^{-3}$), the episodes were of less spatial extend than the previous ten years and no exceedences occurred in the northern part of Europe. There were no European scale ozone episodes with a duration of several days and the

exposure of the European population was only slightly larger than in the previous year. It is believed that this scenario was due to decreases in ozone pre-curser gas emissions.

The first section of the report describes the calculations of energy savings and emission reductions while subsequent chapters comprise descriptions of the modelling system and how it performs for the base year, the results of the project and recommendations for future studies.

Emission estimation

Energy savings from 2005 to 2020 due to insulation were calculated by comparing a business as usual (BAU) and an improved insulation scenario (IIS). The savings which related to different energy carriers used for the purpose of space heating were assessed for the EU-25 countries as zone averages. The countries were divided into six zones each with their own climate characteristics (figure 1). The analysis included residential and non-residential buildings, renovation activities as well as new buildings.

Figure 1: Map (Reis (2004)) of the EU-25 countries included in this study. Note that Cyprus and Malta have not been taken into account. Countries are divided into climate zones according to: Zone 1: Finland, Sweden; Zone 2: Austria, Belgium, Denmark, France, Germany, Ireland, Luxemburg, The Netherlands, United Kingdom; Zone 3: Greece, Italy, Portugal, Spain; Zone 4: Estonia, Latvia, Lithuania; Zone 5: Poland; Zone 6: Bulgaria, Czech Republic, Hungary, Romania, Slovakia, Slovenia.

The IIS assumed ambitious insulation levels in new buildings (very low energy buildings) and retrofits. The changes in U-values for the BAU and IIS scenarios were taken from ECOFYS (2008) (see table 1), which were based on ECOFYS (2007). Note that the savings only relate to the improvement in insulation levels from a standard level to a more ambitious level (and not the full savings compared to a situation without insulation). The savings also do not include further savings from improved windows, ventilation systems with heat recovery, improved supply systems etc. The average renovation activities (including major improvements of the energy performance of the building) in the EU from 2005 until 2020 were assumed with 2 % of the stock per year. The new building activities were assumed at 1 % of the stock per year. The assumption on energy mix follows ECOFYS (2008). The

Table 1: Thermal conductivity (U-value) ($Wm^{-2}K$) for the business as usual (BAU) and improved insulation scenario (IIS).

Zone	Roof	Wall	Floor
BAU scenario			
1	0.13	0.17	0.17
2	0.23	0.38	0.41
3	0.43	0.48	0.48
4	0.20	0.26	0.29
5	0.23	0.25	0.60
6	0.23	0.35	0.46
IIS scenario			
1	0.12	0.15	0.18
2	0.14	0.18	0.22
3	0.20	0.26	0.58
4	0.15	0.17	0.21
5	0.16	0.18	0.23
6	0.18	0.20	0.26

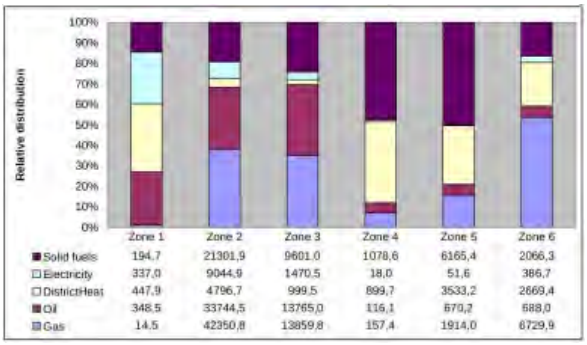

Figure 2: Energy reductions (GWh) per carrier by 2020.

resultant energy reduction by 2020 is displayed in figure 2.

The corresponding emission reductions are assumed to affect main air pollutants comprising particulate matter (PM), sulphur dioxide (SO_2), nitrogen oxides ($NOx = NO + NO_2$), carbon monoxide (CO) and organic compounds (VOC: volatile organic compounds). The emission reductions are based on emission factors which describe the emission rate of a pollutant for a specific activity e.g. kilogram of NO per MWh energy produced by oil combustion. The usage of emission factors pre-assumes a linear dependency between the emission and the intensity of a given activity, i.e. emission = activity × emission factor. The uncertainty in the emission factor, therefore, translates directly to an uncertainty in the emission.

The uncertainty in the calculated emissions significantly depends on the type of pollutant. Of the pollutants considered here SO_2 emissions can be estimated with a high degree of certainty. The fuel sulphur content which may be determined accurately is almost completely oxidized during combustion and consequently all the sulphur of the fuel is released in the flue gasses as SO_2. Emissions of the other pollutants are caused by incomplete combustion (CO and VOC) and chemical reactions during combustion and emission (PM, NO_x). These emissions are therefore, amongst other factors, in addition to the fuel content dependent on the type of combustion (e.g. for oil normal or tangential firing), type of combustion vessel (e.g. low NO boiler), type of fuel (e.g. oil type) and the level of combustion control. Other uncertainties regard the degree of maintenance, e.g. CO emissions from oil combustion may increase by a factor of 10 to 100 if the combustion unit is not properly operated. Similarly, boiler load may af-

Table 2: Average emission factors ($kg\,(MWh)^{-1}$) calculated using the assumptions described in the text. Bituminous and subbituminous coal combustion was considered and it was assumed that 95 % of fuel sulphur was emitted as SO_2.

Specie	Oil	Gas	Coal
SO_2	1.63	$9.1{\cdot}10^{-4}$	2.05
NO_x	0.36	0.19	0.85
CO	$5.30{\cdot}10^{-2}$	0.12	0.86
PM	$1.02{\cdot}10^{-1}$	$1.15{\cdot}10^{-2}$	0.95
NMVOC	$5.0{\cdot}10^{-3}$	$6.2{\cdot}10^{-3}$	$5.1{\cdot}10^{-3}$

fect emissions of filterable particles during combustion of residual fuel oil.

The energy savings are expressed as mean values over a given zone and include both residential governmental and industrial buildings (specific percentages of residential to non-residential contributions to the energy savings are not known to this study). They therefore include both small residential burners and large industrial burners. Furthermore, some countries apply strict combustion control (e.g. Denmark) while others in the same zone do not have as strict a control. Therefore, average (taken over the uncertainty factors described above) emission factors, facilitate the most precise calculations of emissions in this study. Emission factors for oil, gas and coal combustion were compiled from the US Environmental Protection Agency AP42 (Wang, 1999; U.S EPA, 2009). Averages were taken over boiler types and fuel types. When quality indicators were present, higher-quality data were used. For oil heating, the values used in the conversion from lb per 10^3 gal to kg per MWh were 140 MMBtu per 10^3 gal for No. 2 and distillate fuel oil and 150 MMBtu per 10^3 gal for other types. For gas an average heating value of 1.020 Btu scf^{-1} were used in conversions from lb per 10^6 scf to kg $(\mathrm{MWh})^{-1}$ and for coal an average heating value of 26 MMBtu per ton were used in the conversion from lb per ton to kg $(\mathrm{MWh})^{-1}$ (see table 2 and figure 3 for the resultant average emission factors and their relative distribution).

Electricity is mainly generated by combustion of coal and gas and by nuclear power. Using the EEA electricity projections for 2020 (EEA, 2002) for the baseline scenario in the EU-25 zones gives a forecast of the fuel mix. According to the EEA projections electricity production will be associated with 38.9 % coal and lignite combustion, 21.3 % nuclear power generation, 20.4 % natural and derived gas combustion, 22.5 % renewable energy sources (solar, wind, wood and waste) and 1.9 % oil combustion. Assuming that this energy mix will be applicable in all the zones we associated the energy savings due to changes in electricity usage by 2020 with the fuel types. As an example consider zone 1 where the total energy saving due to electricity by 2020 is 337 GWh. Since some fuel types do not lead to emissions this saving is split into fuel types according to the above percentages and may then be used for calculation of the total emissions of air pollutants. Note that we assumed that nuclear power and renewable sources did not contribute to the emissions (lacking information on emission factors). The resulting energy savings, resolved according to fuel type, were added to the energy savings for oil, gas and coal in order to get the total emission reduction for these fuel types.

Table 3: Zone averaged fuel mix (%) for district heating (only oil, coal and gas) by 2020 ((EEA, 2005)) for cogeneration plants.

Zone	Oil	Gas	Coal
1	16.8	25.0	25.8
2	0.0	41.1	1.0
3	18.7	39.7	0.1
4	0.0	83.3	16.7
5	0.0	0.0	92.0
6	0.0	28.8	47.3

For district heating systems in Europe,

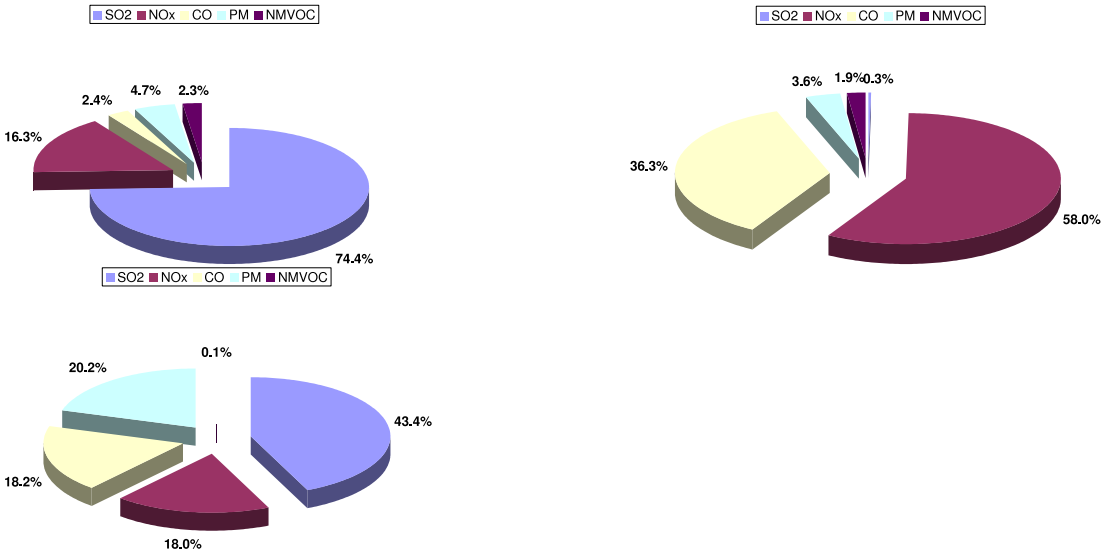

Figure 3: relative distribution of pollutants from combustion of oil (top left), gas (top right) and coal (lower left). The values are based on the average emission factors displayed in table 2.

Table 4: Zone and fuel type specific total energy savings (GWh) where savings in electricity and district heating due to insulation by 2020 (based on EEA projections of fuel mix (EEA, 2002, 2005)) has been recalculated in terms of oil, gas and coal. The total energy saving by 2020 due to insulation is 172 TWh.

Zone	Oil	Gas	Coal
1	430	195	441
2	34073	46165	25293
3	13980	14556	10367
4	116	911	124
5	765	2019	9436
6	789	7577	3480

heat is mainly obtained via cogeneration plants and heat only plants. Nuclear, solar and geothermal sources also exist but do not emit significant amounts of air pollutants and are therefore not included here.

Using 2005 values and assuming that cogeneration plants are still dominating the European district heating system in 2020, the zone-specific fuel type input to cogeneration plants can be derived from EEA-EN20 (EEA, 2005) (it is assumed that solid fuels consists mainly of coal) (table 3). The energy savings in district heating due to insulation may be estimated by dividing them between fuel types (see table 4 for the total electricity and district heating related savings).

The total emissions were then calculated based on the above assumptions. The electricity and district heating savings were added to the oil, gas and coal savings. The changes in total emissions from oil, gas and coal based on the energy savings and the emission factors were then produced. Figure 4 displays the resultant emission savings in each zone. The total reduction in air pollutant emissions in 2020 then becomes about $368\,10^3$ t. The emis-

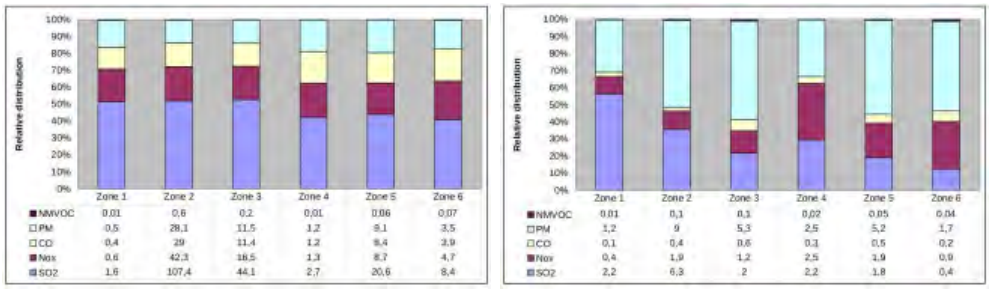

Figure 4: Absolute (10^3 t, left) and relative (%, right) emission reductions corresponding to the energy reductions in figure 2.

sion savings corresponding to reductions in energy usage due to insulation were then converted into relative terms by dividing by the yearly emissions of the species for each zone. The total emissions were calculated by summing over all emission inventory (see section "modelling" for a description of the inventory) contributions from power generation and residential combustion. The values for each country was then added to reflect the total yearly emissions in a given zone (see figure 4 for the relative savings).

In order to reach realistic estimations of the emission reductions it is neccessary that the energy savings as well as the emission reduction calculations include assumptions about the fuel mix by 2020. Therefore, there is a background emission change (but not in the energy savings estimation) in the period 2009-2020 which is not directly related to insulation but relates to the changes in fuel mix used in power generation. In order to evaluate the importance of this assumption the emission reductions were recalculated based on the present fuel mix for power generation. It was found that the total (all zones included) emission change was modest and corresponded to about 0.005 % in NO_x, 0.02 % SO_2, 0.003 % in CO and 0.05 % in PM while volatile organic compounds were unaffected. Therefore, the emission reductions are directly related to the effect of insulation in this study.

Modelling

Model description

The Comprehensive Air-Quality Model with Extensions (CAMx Environ (2010)) was used to describe the spatial and temporal development of the gaseous and particulate pollutants. The model was used with the carbon bond mechanism IV gas-phase chemistry (Gery et al. (1989); Carter (1996)) and the Euler-Backward Iterative kinetics solver (Hertel et al. (1993)). For the aerosols the coarse and fine (CF) option was used including aqueous-phase sulphate and nitrate formation in cloud water (Chang et al. (1987)) and condensation of semi-volatile organic gases to secondary organic aerosols (Strader et al. (1999)). The thermodynamic equilibrium between gas and aerosol phases was modelled using the ISORROPIA mechanism (Nenes et al. (1998)). For advection the Piecewise Parabolic Method (PPM, Colella and Woodward (1984)) was used.

Emission inventory

In correspondence with the energy reduction calculations an emission inventory with a 2005 base year was used. The inventory was developed by Kuenen et al. (2010) and covers Europe with a resolution of 0.06125° longitude and 0.125° latitude. It contains annual values for nitrogen oxides, sulphur dioxide, carbon monoxide, particulate matter and volatile organic compounds which were scaled to obtain hourly variability and interpolated to the model grid. Biogenic emissions of isoprene, monoterpenes and other biogenic volatile organic compounds are calculated dynamically based on the inventory values.

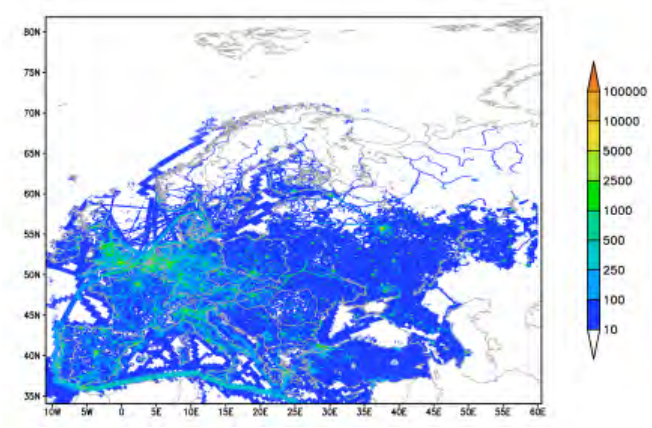

Figure 5: Total NO_x ($NO+NO_2$) emissions (ton per year) from the emission inventory used in this study. Emission lines in marine areas are ship tracks while lines on land surface mainly reflects major roads.

Figure 5 displays the nitrogen oxide emissions as an example.

Input meteorology

The base year for the emission inventory and the energy reduction estimation was 2005. Together with 1998 the annual averaged surface temperature in 2005 was the greatest ever recorded (NOAA (2010)). In order to avoid chemistry signals related to the extraordinary heating we used meteorological input for the year 2009. In order to focus on the effect of insulation, the development of the European climate between 2005 and 2020 were not considered in this study and the meteorological fields of 2009 were assumed to be representative of the period. The 2009 winter and autumn were relatively cold in most of Europe while spring and summer were relatively warm (EEA (2010b)).

The meteorological input (wind, temperature, surface pressure, humidity, precipitation and turbulent kinetic energy) to

CAMx was extracted from the archives of the operational short range weather forecast model, DMI-HIRLAM (High Resoluation Limited Area Model) (Yang et al. (2005,b)), used at DMI. The CAMx simulations were made with two days spin-up starting from "day −2, 00 UTC" with basic initial conditions, meteorology and emissions based on the corresponding 00 UTC DMI-HIRLAM-T15 (where T15 refers to the area displayed in figure 6 with 0.15° horisontal resolution and 40 levels in the vertical with the top at 10 hPa) simulation. The fields were extracted every hour for the first 24 h. The CAMx run dumps the model state after the end of the 24 h run. This state is used as initial conditions for the following 24 h period starting at 00 UTC at "day −1" with meteorology and emissions based on the "day −1, 00 UTC" T15 simulation. The new CAMx run also dumps the state after the end of the 24 h run. This state is used as initial state for the "day 0, 00 UTC".

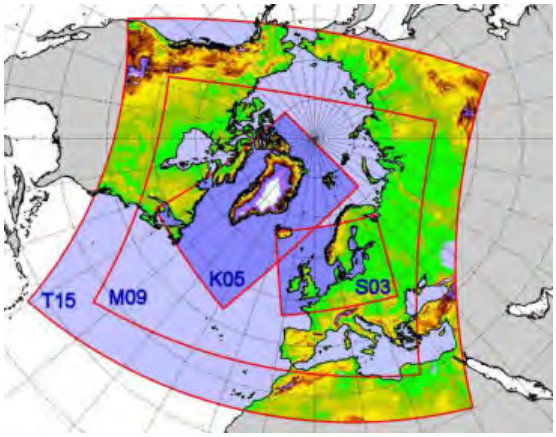

Figure 6: DMI-HIRLAM model areas since May 2009.

Evaluation of chemical predictions

The model system used in this study has been validated on a daily basis in the context of the European project GEMS (Global and regional Earth-system (Atmosphere) Monitoring using Satellite and in-situ data: `http://gems.ecmwf.int/about.jsp`). The current verification scores as compared to other European air-quality models can be seen on the project web page (`http://gems.ecmwf.int/d/products/raq/`; CAC model). The system generally perform as well as other model systems. An evaluation of the monthly mean performance, however, is of special interest in this study. The evaluation was made for ozone since this is where the largest amount of observational data was available and because it is a secondary specie which is sensitive to changes in both NO_x and organic compounds, and therefore its evaluation represents aspects of the chemistry scheme as a whole.

Data were downloaded from the World Meteorological Organization database World Data Centre for Greenhouse Gases (WDCGG (2010)). For the year, 2009, data from 12 stations were available. Four of these were mountain stations, and therefore discarded, since the horizontal and vertical resolution of the model as applied here does not account for mesoscale mountain circulations or emissions. Therefore, a comparison to observations at such locations is not representative of the model performance. Furthermore, concentration levels at particular mountain stations are not of relevance for this study, since most of the European population live in urbanized areas away from mountainous regions. On the remaining eight stations (see table 5) monthly average, monthly average daily maximum and monthly average daily minimum ozone concentrations were considered.

Statistical quantities

The statistical quantities follow those described by Mosca et al. (1998) and is repeated here for completeness. The mean value of a quantity p was calculated as $\bar{\mathrm{p}} = \frac{1}{\mathrm{n}} \sum_{i=1}^{\mathrm{n}} \mathrm{p}_i$ where n is the number of data points and p is the time series to be averaged, here taken as the model predictions. The bias is then calculated as $\overline{\mathrm{p}-\mathrm{o}}$, where o denotes observations. The normalised mean square error is defined as NMSE $= \frac{1}{\overline{\mathrm{o}}\overline{\mathrm{p}}} \sum_{i=1}^{\mathrm{n}} (\mathrm{o}_i - \mathrm{p}_i)^2$ and the linear correlation coefficient follows from $\mathrm{r} = \sum_{i=1}^{\mathrm{n}} (\mathrm{o}_i - \bar{\mathrm{o}})(\mathrm{p}_i - \bar{\mathrm{p}}) / \sum_{i=1}^{\mathrm{n}} (\mathrm{o}_i - \bar{\mathrm{o}})^2 (\mathrm{p}_i - \bar{\mathrm{p}})^2$. The standard deviation is defined as $\mathrm{Std_p} = \sqrt{\frac{1}{n} \sum_{i=1}^{\mathrm{n}} (\mathrm{p}_i - \bar{\mathrm{p}})^2}$ while the fractional standard deviation is given as $\mathrm{FSD} = 2(\overline{\mathrm{Std_p}} - \overline{\mathrm{Std_o}}) / (\overline{\mathrm{Std_p}} + \overline{\mathrm{Std_o}})$ and the fractional bias is likewise defined as $\mathrm{FB} = 2(\overline{\mathrm{p}} - \overline{\mathrm{o}}) / (\overline{\mathrm{p}} + \overline{\mathrm{o}})$. The figure of merit is defined as $\mathrm{FM} = 100\,\% (\sum_{i=1}^{\mathrm{n}} \mathrm{Min}(\mathrm{p}_i, \mathrm{o}_i)) / \sum_{i=1}^{\mathrm{n}} \mathrm{Max}(\mathrm{p}_i, \mathrm{o}_i)$. The confidence level of the bias is given as $\mathrm{Conf} = \mathrm{t}(\beta)\ \mathrm{Std_{bias}}/\mathrm{n}$ where t is the β^{th} percentile of the t-distribution defined on n-1 degrees of freedom. Using the null hypothesis $\mathrm{H_0}$: r= 0, i.e the predicted and observed time series are uncorrelated, the test-statistic $\mathrm{t}_c = \mathrm{r}\sqrt{n-2}/\sqrt{1-\mathrm{r}^2}$ which is t-distributed gives a confidence level on which we can reject $\mathrm{H_0}$.

The monthly mean scatter plots in figure 7 along with the statistical quantities

in table 7 summarize the global performance of the model (paired data in space and time at all available stations and all available times). When interpreting these results it is important to stress that rather few measurement stations were available, i.e. parts of Europe are not represented in the analysis, and measurement stations located in mountainous regions will likely degrade the statistical scores due to insufficient resolution of mesoscale circulations.

For all the global data sets about 70 % of the points are located within ±1 standard deviation of the mean, and the the mean and median values are close. Hence, the data series may be assumed to be normally distributed, and the linear correlation and other statistical quantities sensitive to the underlying distribution may be calculated without prior data transformation.

The fractional bias and standard deviation are dimensionless, symmetrical and bounded quantities with values between −2 (extreme under prediction) and +2 (extreme over prediction). Values of −0.67 (0.67) corresponds to under prediction (over prediction) by a factor of two and model predictions close to zero are relatively free from bias. The low values of the fractional and absolute bias indicate good monthly mean model performance. Indeed by comparing bias and correlation to state of the art air-quality models (e.g. the Monitoring atmospheric composition and climate web page: `http://macc-raq.gmes-atmosphere.eu/somi\_OF.php`) it is found that the model performs well in both parameters for both monthly mean, maximum and minimum.

The mean, standard deviation and variance of the model and the observations are also in good correspondence for both

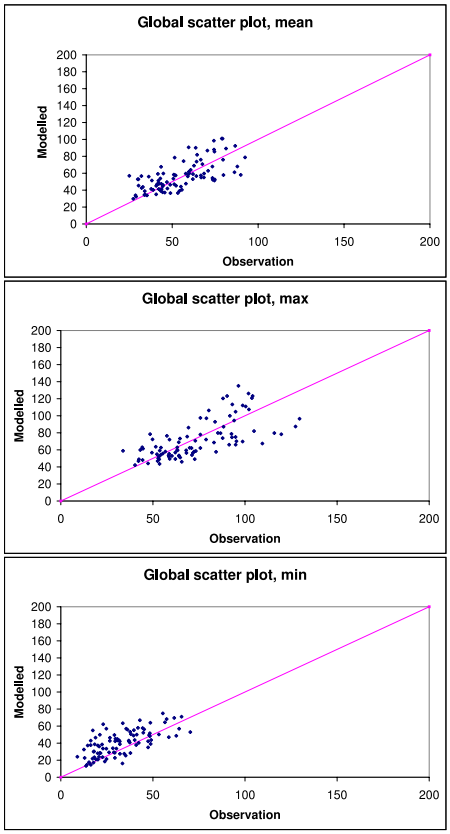

Figure 7: Global scatter plots of predicted mass concentrations vs. observations on the eight measurement stations for the monthly mean, monthly averaged daily maximum and monthly averaged daily minimum ozone values ($\mu g\,m^{-3}$). Corresponding statistical quantities are displayed in table 7

Table 5: Coordinates of available measurement stations along with abbreviations used in the text.

Station	Lon.	Lat.	Abb.
K-puszta	19.55E	46.97N	St1
Rucava	21.17E	56.16N	St2
Dobele	23.19E	56.37N	St3
Zingst	12.73E	54.43N	St4
Westerland	8.32E	54.93N	St5
Zoseni	25.54E	57.08N	St6
Vindeln	19.77E	64.25N	St7
Waldhof	10.77E	52.80N	St8

the monthly mean, monthly averaged maximum and monthly averaged minimum values while the fractional bias is close to zero. The model tends to over predict the monthly averaged minimum value. However, the values are well within an acceptable range by comparison to other models.

Figures 8 to 10 give an overview of the results on individual stations. For each station mean, bias, normalised mean square error, linear correlation, standard deviation, fractional bias, figure of merit, 95 % confidence interval of the bias, and t-statistic for the monthly mean, monthly mean maximum and monthly mean minimum were computed.

For the mean value calculation the stations were ranked by assigning the best rank to the statistic containing the best performance (standard deviation not included in the ranking), e.g. the station with the lowest bias will be assigned a one while the station with the highest bias will be assigned an eight. Each statistical parameter bears the same weight in this scheme. By adding the ranks for each statistic, an overview of the performance at the stations is generated (table 6). The stations at which the model performs best is St5, while the lowest score is found at St6 (table 5). The Zoseni station (St6) is located close to the Vidzeme hills and valleys which may affect the performance at that station.

There are both positive and negative biases. The largest absolute value ($14.38\,\mu\mathrm{g\,m^{-3}}$) was found at Waldhof while the lowest ($1.26\,\mu\mathrm{g\,m^{-3}}$) was found at Dobele. The largest correlation (0.93) was found at Westerland while the smallest one (0.61) was likewise found at Dobele. Comparing the bias and the correlation of the monthly mean ozone concentrations to corresponding values for other models (`http://gems.ecmwf.int/d/products/raq/`; CAC model) it is found that the model performs well in the sense that the largest bias and smallest linear correlations are well within the spread of the other models. It may also be noted that the emission inventory as well as the measurements themselves are also associated uncertainty.

Figure 8: Monthly mean ozone concentration ($\mu g\,m^{-3}$) at eight measurement stations (table 5) along with modelled values from the baseline and emission simulations.

Figure 9: Monthly mean maximum ozone concentration ($\mu g\,m^{-3}$) at eight measurement stations (table 5) along with modelled values from the baseline and emission simulations.

Figure 10: Monthly mean minimum ozone concentration ($\mu g\,m^{-3}$) at eight measurement stations (table 5) along with modelled values from the baseline and emission simulations.

Table 6: Mean statistics for eight measurement stations. Mean refers to an annual average ($\mu g\,m^{-3}$), Std: standard deviation, Conf: 95 % confidence interval of the bias, FB: fractional bias, Fsd: fractional standard deviation, FM: figure of merit (%), NMSE: normalised mean square error, r: Pearson's correlation coefficient and t_c; the corresponding t statistic. Ranking of the stations along with the total score in parenthesis is also displayed.

Specie	**St1**	**St2**	**St3**	**St4**	**Specie**	**St5**	**St6**	**St7**	**St8**
Mean Obs	58.90	51.10	49.85	55.23	**Mean Obs**	63.00	57.47	51.83	48.99
Mean Mod	53.25	59.20	51.10	64.23	**Mean Mod**	67.40	48.28	45.95	63.37
Std Obs	21.75	14.14	12.75	16.43	**Std Obs**	17.45	16.87	15.16	17.37
Std Mod	13.61	5.35	7.75	19.58	**Std Mod**	24.62	8.11	6.99	23.94
Bias	−5.65	8.09	1.26	8.99	**Bias**	4.39	−9.22	−5.88	14.38
Conf	0.36	0.22	0.29	0.14	**Conf**	0.20	0.39	0.33	0.16
FB	−0.10	0.15	0.02	0.15	**FB**	0.07	−0.17	−0.12	0.26
Fsd	−0.87	−1.50	−0.92	0.35	**Fsd**	0.66	−1.25	−1.30	0.62
FM	79.19	81.45	86.28	85.85	**FM**	87.41	79.52	80.90	77.31
NMSE	0.07	0.07	0.04	0.04	**NMSE**	0.03	0.08	0.06	0.10
r	0.74	0.42	0.61	0.91	**r**	0.93	0.70	0.75	0.92
$\mathbf{t_c}$	3.48	1.38	2.17	6.79	$\mathbf{t_c}$	7.93	3.08	3.53	7.53
Rank	4(38)	6(46)	20(32)	3(33)	**Rank**	1(15)	7(51)	3(33)	5(40)

Table 7: Annual mean, annual mean daily maximum (Max) and annual mean daily minimum (Min) ozone mass concentrations ($\mu g\,m^{-3}$) (with 95 % confidence intervals) along with global statistical quantities. FBias: fractional bias, FStd: fractional standard deviation, Corr: linear pearsson correlation coefficient.

Statistic	**Mean**		**Max**		**Min**	
	Obs	**Model**	**Obs**	**Model**	**Obs**	**Model**
Points	93	93	93	93	93	93
Mean	54.68±0.10	56.68±0.11	73.44±0.14	71.62±0.14	32.79±0.10	40.57±0.10
Max	92.40	101.50	129.62	135.11	70.29	74.95
Min	25.03	29.74	33.77	42.15	8.98	13.29
Median	52.24	54.37	69.96	63.63	30.72	42.03
Fractile 75 %	66.86	62.87	91.38	79.72	41.88	50.20
Fractile 95 %	83.53	90.36	106.93	120.57	59.95	65.60
Std	16.80	17.02	21.35	22.29	14.22	14.74
Variance	282.23	289.84	456.03	496.83	202.11	217.16
FStd		0.013		0.043		0.036
Bias		2.00±0.23		−1.82±0.37		7.78±0.25
FBias		0.036		−0.025		0.21
Corr		0.67		0.68		0.67

Effects on regional concentration levels

In this study we have quantified the effect of insulation changes on air-quality. Although the method applied accurately describes the response to emission reductions it should be noted that scaling the results to other emission reductions is not readily possible due to non-linearity of the chemical and meteorological processes. For some of the primary pollutants the response may be considered linear for small perturbations in the emissions (as is considered here) and the impact may be scaled directly from the baseline simulation. For secondary pollutants such as ozone or a large fraction of PM which are generated by non-linear interactions among precursers the response is more complex and requires the full non-linear chemical equations.

Criteria air pollutants

Nitrogen oxides

Nitrogen oxides are a group of highly reactive gasses including NO, NO_2 and HNO_3. HNO_3 is mainly formed from the reaction of NO_2 with water vapor in the atmosphere, and NO is quickly converted to NO_2 after emission. Hence, it is appropriate to use NO_2 and NO (denoted NO_x) as a primer for the group of nitrogen oxides. Natural sources of NO_x include lightning, forest fires, volcanoes and soil microbes. Generally, it is produced during high-temperature combustion of fossil fuels. Therefore, motor vehicles along with industrial, electrical and residential facilities are the main emitters of NO_x.

Exposure to nitrogen oxides has been linked with airway inflammation and other respiratory effects in healthy people and enhanced symptoms for people suffering from asthma. Reactions with ammonia and water vapour (and other compounds) lead to formation of small particulates which upon inhalation have been shown to cause or worsen respiratory diseases and enhance heart diseases. HNO_3 is a strong acid which upon dissolution in aerosols, clouds and fog acts to acidify rain and increase acid deposition to soil and water surfaces. It is harmful to ecosystems, including trees, animals and aquatic species as well as some types of buildings. Figure 11 displays the seasonally averaged (spring months: March, April, May; summer months: June, July, August; autumn months: September, October, November; winter months: December, January, February) NO_x concentration near the surface. The average NO_x lifetime is about a day and therefore source points show up clearly in the seasonal mean and ship tracks are visible in all seasons. A band of increased NO_x concentration extending from mid-England to Poland is visible as a combination of ship track emissions and emissions from urban areas. Winter time values are generally higher than during summer, consistent with decreased photolysis during the winter season.

Figure 11 also displays the seasonally averaged differences for NO_x. Generally the zone 2 and 5 countries experience the largest decrease. During spring and summer the reduction in near-surface mass concentration over Poland and England

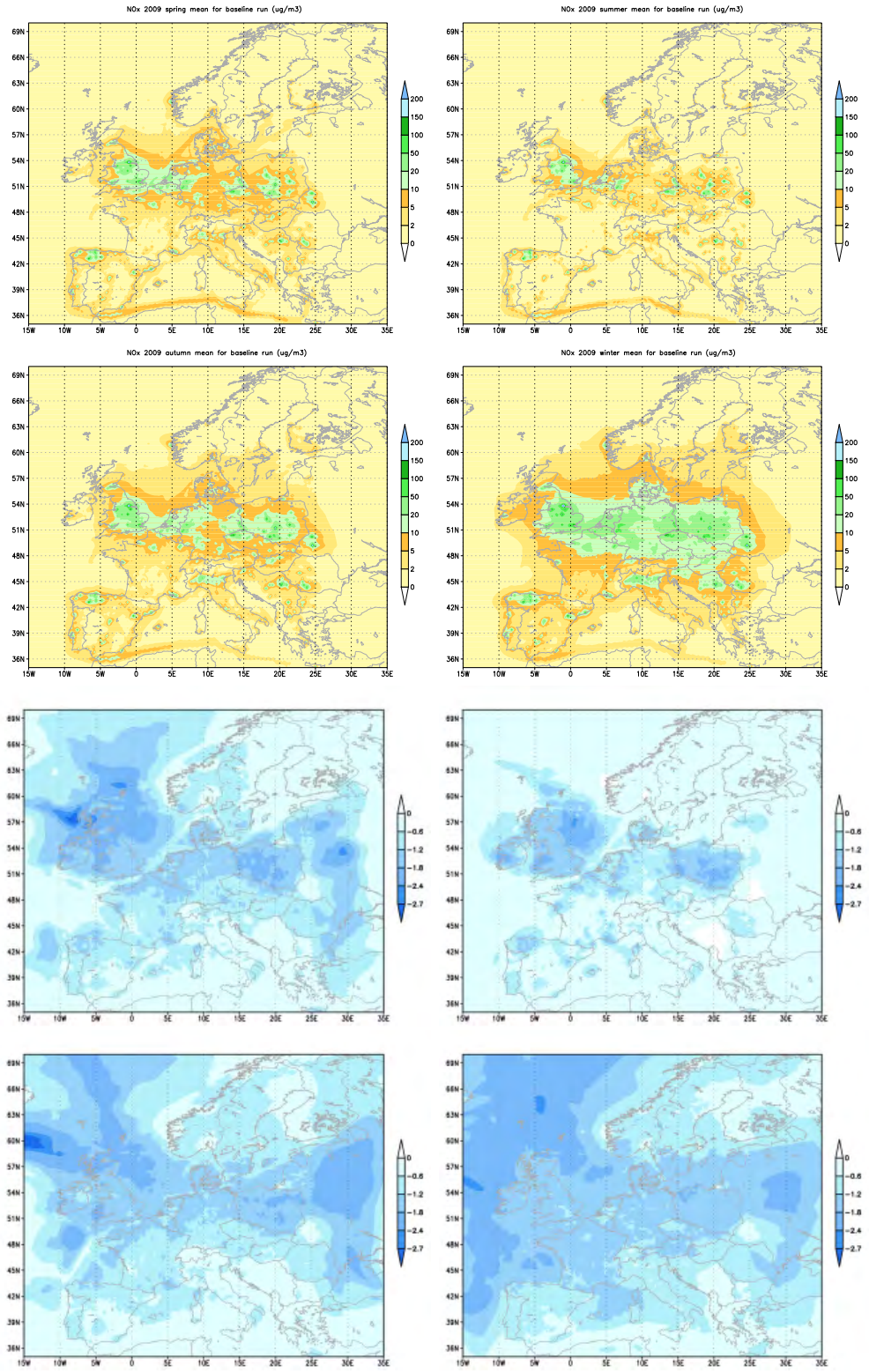

Figure 11: The uppermost four plots display spring, summer, autumn and winter-time averages of near-surface NO_x concentration ($\mu g\,m^{-3}$) respectively. The lowermost four plots display the corresponding relative differences between the baseline and reduced emission simulations (%). Negative values correspond to reduced values.

reaches more than 2 % while the rest of the countries are associated with reductions of between 1.2 % and 1.8 %. During autumn and winter the reductions level out and become more homogeneously distributed. Comparing to the relative emission reductions (figure 4) it is found that the largest response (sensitivity) is found in zone 5 (Poland) where the emissions changed 1.76 %.

Sulphur dioxide

SO_2 is the second most common air pollutant in urbanised areas of Europe, and in the industrialized northern Hemisphere the anthropogenic emissions are about five times larger than the natural. It is an acidic gas which is naturally formed by marine plankton, bacteria, plants and by geothermal sources. The anthropogenic component is mainly formed by combustion of sulphur-containing fuels such as coal or oil (see section Emission estimation on page 5) extraction of gasoline from oil, and industrial facilities such as petroleum refineries.

In the atmosphere SO_2 is oxidized to liquid sulphuric acid (H_2SO_4) in the presence of water e.g. in cloud droplets and to particulate sulphate (SO_4^{2-}) in dry conditions. Sulphate aerosols are a major part of the acid deposition problem through incorporation in rain drops and sedimentation of particulates. They also affect visibility and have adverse health effects, including inflammation of the lungs upon inhalation of aerosols with diameters about 0.1 μm to 1 μm. SO_2 exposure may cause irritation of eyes and lungs and may lead to allergic reactions and asthma in sensitive groups. Long-term exposure to high levels of the gas and particulate phases may cause respiratory disease and enhance heart illness, and is associated with premature death (EEA (2007)).

Figure 12 displays the modelled seasonally averaged SO_2 concentration near the surface. The atmospheric lifetime is about one day. Hence, individual source points are clearly seen in the figures, as is ship tracks in the North Sea and the Mediterranean. Major emitters are mainly located within zone 5 and 6 along with England and Spain. Figure 12 displays the seasonally averaged differences between the baseline and the reduced emission simulation in near-surface concentration of SO_2. Zone 2 generally experiences a decrease between 6 % and 8 %. In spring and summer the largest decrease is found over Belgium, England, Scotland and Ireland while during winter the response is more homogeneously distributed. Local maxima between 8 % and 10 % reductions are found during autumn over England, Scotland and Ireland. Poland (Zone 5) experienced a reduction between 2 % and 4 %.

Carbon monoxide

CO is the most common air pollutant in the urbanised areas of Europe, where typically 95 % of the emissions are of anthropogenic origin. It is generally formed during incomplete combustion of carbon containing fuel and through chemical reactions between trace gases in the atmosphere. Natural sources include volcanoes, forest fires and photochemical reactions in the troposphere while anthropogenic sources mainly include vehicle (cars, busses, aircraft, locomotives etc.) exhaust, industrial processes and residen-

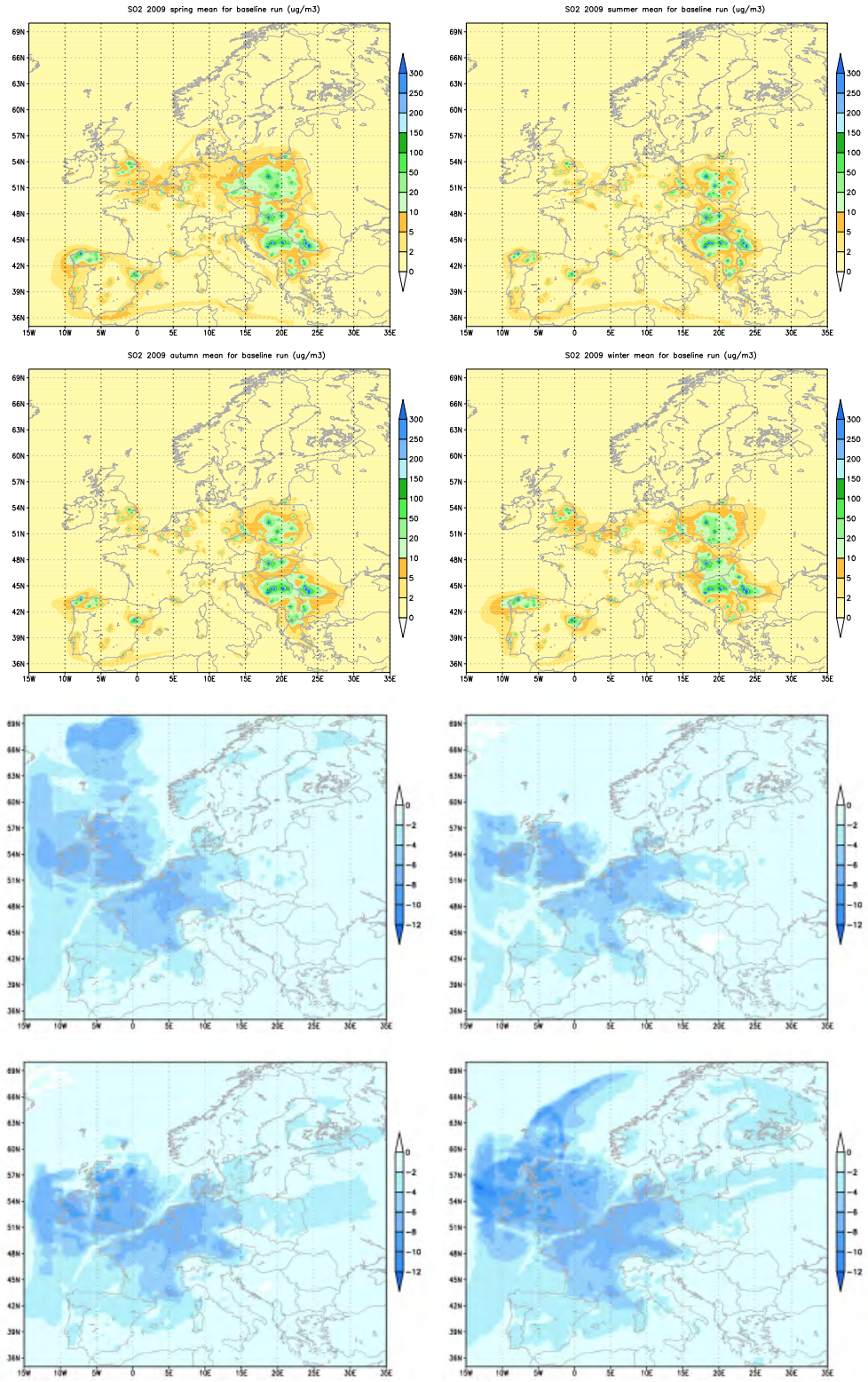

Figure 12: The uppermost four plots display spring, summer, autumn and winter-time averages of near-surface sulphur dioxide concentration (μg m^{-3}) respectively. The lowermost four plots display the corresponding differences between the baseline and reduced emission simulations (μg m^{-3}). Negative values correspond to reduced values.

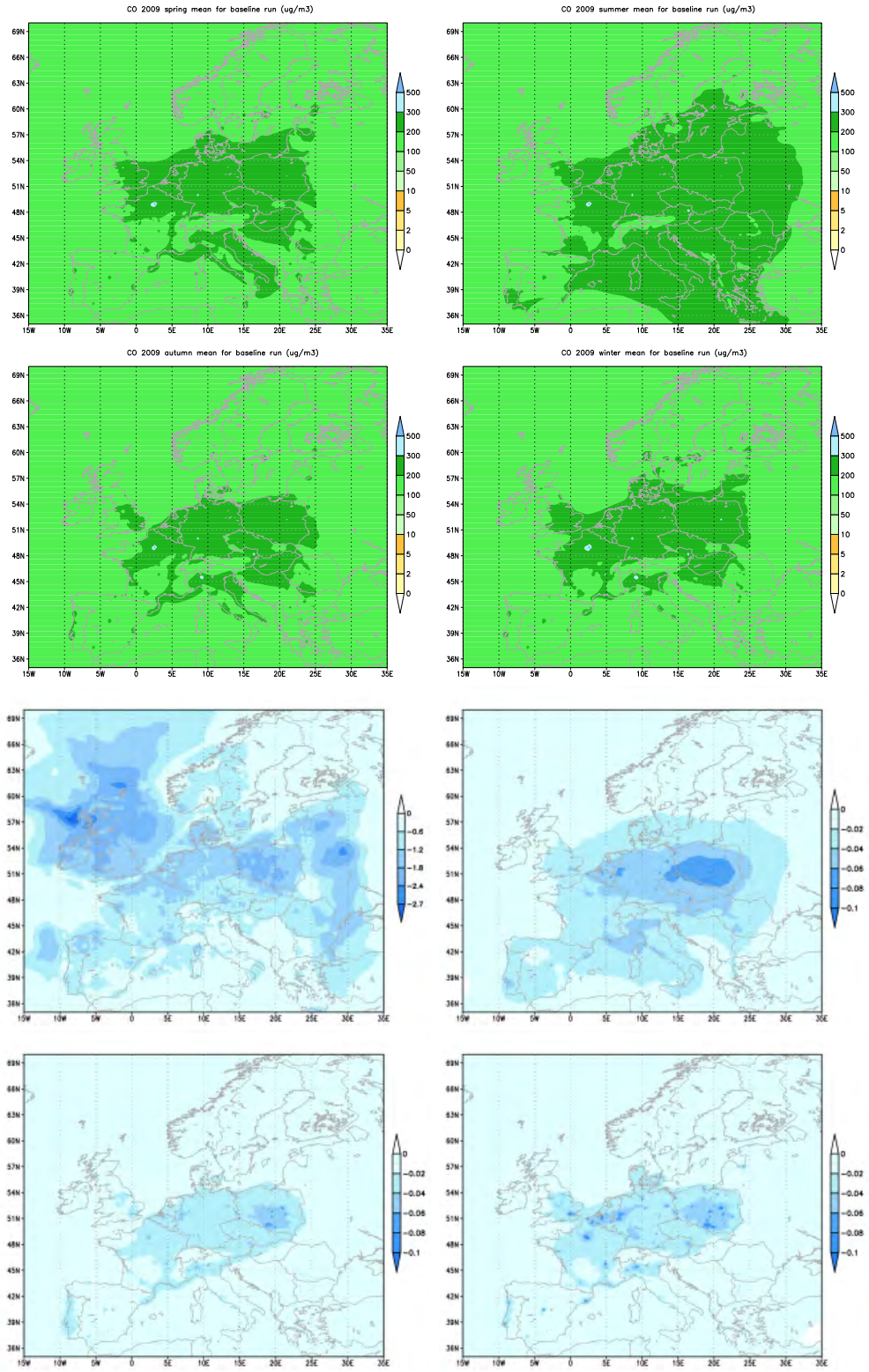

Figure 13: The uppermost four plots display spring, summer, autumn and winter-time averages of near-surface carbon monoxide concentration (μg m^{-3}) respectively. The lowermost four plots display the corresponding relative differences between the baseline and reduced emission simulations (%).Negative values correspond to reduced values.

tial wood burning. In the troposphere CO is oxidized to CO_2, and the average lifetime in Europe is about four months. High doses of CO may be associated with death while moderate doses mainly affect people with heart diseases who experience chest pain, reduced ability to exercise and various cardiovascular effects (EEA (2007)). Seasonal averages of the CO concentration are displayed in figure 13. The long lifetime makes it a relatively well mixed specie. However, individual maxima, likely related to traffic emissions, are visible for e.g. Paris, Barcelona, Warsaw and Vienna. Local maxima are slightly larger during winter consistent with more stagnant conditions and lower inversion heights. During summer increased dispersion acts to extend the field east and south-wards. Seasonally averaged relative differences are displayed in figure 13. The reductions in the CO levels were generally quite low with a maximum decrease of about 0.1 % over major urban source points including London, Paris, Madrid, Barcelona, Lisboa and Riga. The largest decrease was found in winter and spring where a general decrease between 0.06 % and 0.08 % existed over Poland. Zone 2 generally experienced a decrease between 0.06 % and 0.08 % while zones 1,3,4 and 6 showed only point-wise reductions

Ozone

Ozone is a secondary pollutant which forms when NO_x and volatile organic compounds react in the presence of sunlight. VOCs are emitted naturally from plant stomata while anthropogenic sources include chemical solvents, vehicle exhaust and industrial emissions. Tropospheric ozone concentrations have a strong dependency on weather, and increased values can appear anywhere due to transport effects. However, extreme values are associated with stagnant weather conditions, high temperatures and clear skies, and therefore the ozone season typically runs from April to September.

Breathing of ozone is associated with a variety of health effects including inflammation of the lungs and reduced functioning, enhanced bronchitis and asthma and chest pain, irritation of the throat and congestion. Ozone also has detrimental effects on ecosystems and plants including reduced crop yield, and growth, and leaf damages (EEA (2007)). The formation of ozone in the troposphere is bound to NO_x and volatile organic compounds. Local minima are found over urban areas consistent with titration effects of NO. Increased values appear away from the source points in aged air where NO has generally been converted to NO_2. The seasonal variation favours increased values over marine areas in summer time consistent with increased levels of CO and formaldehyde (CH_2O) released by the ocean during summer time.

The seasonally averaged difference in ozone is displayed in figure 14. Generally, the emission reductions led to increased levels of ozone during autumn and winter time while small increases were found during spring and summer. During spring a small decrease of less than 0.5 % were found over Poland while mid-England experienced an increase of about 0.5 % and up to 2 % over individual source points. During autumn the increase in ozone concentration over pre-curser sources increased further and reached up to 3 % during winter. A band of increased ozone

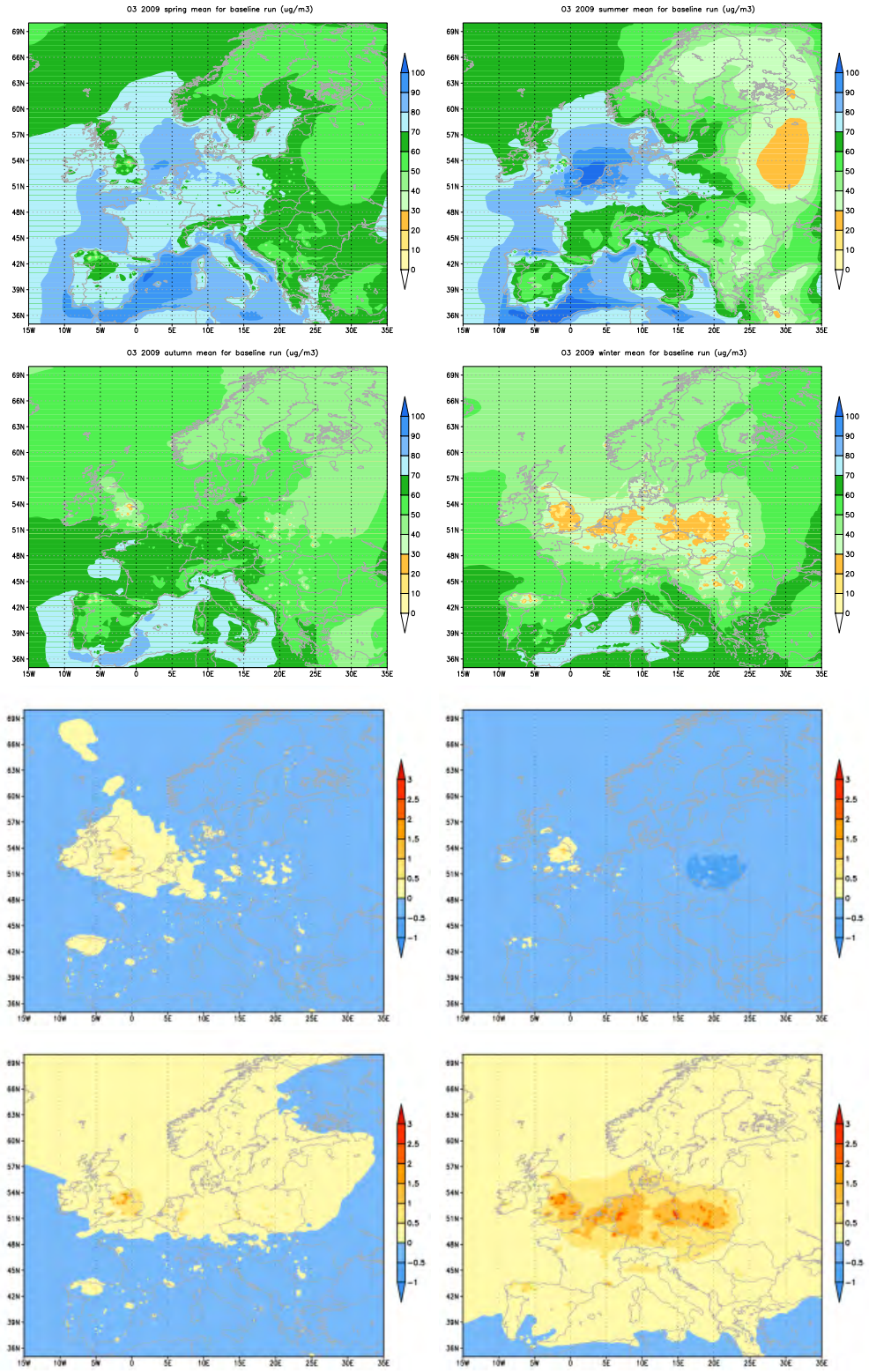

Figure 14: The uppermost four plots display spring, summer, autumn and winter-time averages of near-surface ozone concentration ($\mu g\,m^{-3}$) respectively. The lowermost four plots display the corresponding relative differences between the baseline and reduced emission simulations (%). Negative values correspond to reduced values.

concentration extending from England to Poland was established during autumn and winter where the increase reached 2 %.

Particulate matter

Tropospheric particles occur naturally through emissions from volcanoes, forest fires, vegetation and sea salt along with secondary nucleation in trace gases. The anthropogenic component mainly arise from combustion of fossil fuels in vehicles, power plants and industries. Characteristic aerodynamic diameters range from less than 10 nm to more than 10 μm. Composition depends on the origin of the particles, but is generally dominated by sodium chloride, sulphate, nitrate, ammonium, organic constituents and mineral oxides. Secondary particles may be generated through oxidation of anthropogenic sulphur and nitrate oxides (sulphuric acid, nitric acid, ammonium salts).

Health effects generally depend on particle sizes and have been associated with asthma, lung cancer, cardiovascular disease and premature death. Smaller particles (less than 100 nm) may penetrate cell membranes in the lungs and enter other organs while larger particles (e.g. 10 μm) are less hazardous despite their larger mass (EEA (2007)). Mean values and relative differences for each season are displayed in figure 15. The largest reductions were found during spring and summer time where England experienced a general reduction of 4 %-5 % and over France, Germany, Belgium and the Netherlands the reduction was about 3 %. Point-wise reductions of up to 6 % were found over major urban sources including Leeds and Marseilles during spring. During autumn the point-wise and general reduction becomes smaller, and for the winter season a general reduction of about 2 %-3 % persists.

Uncertainties associated with the modelling

Chemical fields derived from numerical models are prone to noise. Here we distinguish between two main types: numerical noise and noise associated with the non-linearity of the governing equations.

Numerical noise arises due to limitations in the numerical solution of the model equations and is typically manifest in the computational results as oscillations near steep gradients. Such undershoots and overshoots may lead to negative or unrealistic concentration levels and loss of mass conservation depending on how such modes are damped or removed. Given the small perturbations in emissions (less than 10 %) used in this study special attendance should be given to the signal to noise ratio. The CAMx model as used in this study employs the piecewise parabolic method (see section Modelling on page 10) for solving the advection equation. This method is strictly mass conserving and monotonic and contains very low diffusion. Hence, the numerical noise level due to advection is expected to be low. However, statistical tests for the significance of the signal must still be produced. Other numerical noise issues may arise due to inconsistencies between the meteorological driver and the chemical transport model (Korsholm et al. (2009)) leading to less precise predictions of the chemical fields. In this study a meteorological coupling interval of 1 hour was used, and relative to the monthly to seasonal scales under consideration this is

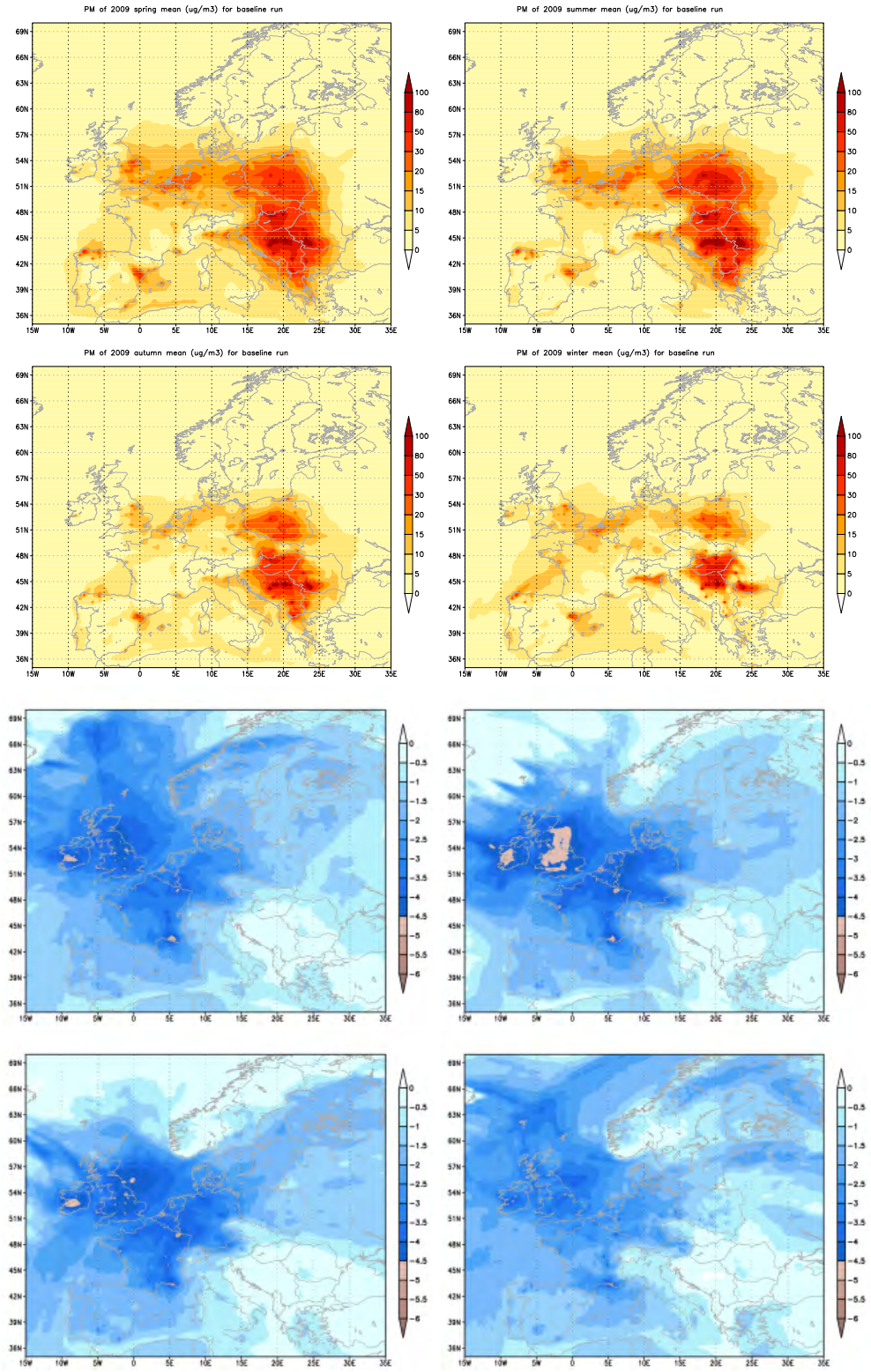

Figure 15: The uppermost four plots display spring, summer, autumn and winter-time averages of near-surface PM concentration ($\mu g\,m^{-3}$) respectively. The lowermost four plots display the corresponding relative differences between the baseline and reduced emission simulations (%). Negative values correspond to reduced values.

adequate. The comparison with measurements served to evaluate whether such issues are present in the model.

The quantification of the effect of insulation on air quality requires solution of the full non-linear set of equations describing chemical and physical transformations of the pollutants. Since the governing chemical and meteorological equations are non-linear, comparison between emission reduction simulations may show spurious random results, i.e. changes are made in the boundary conditions of an inherently chaotic system. This is of special importance for the secondary species such as ozone and secondary PM. In general the perturbations made to the emissions in this study are small and it is expected that the non-linear response of the system is significantly smaller than the linear one. However, non-linear dynamical noise signals cannot be readily disregarded.

Averaging the fields in time will filter out the random non-linear signal. However, the averaging time must be chosen with some care. Although seasonal time scales must be considered long as compared to the characteristic time scales for individual chemical reactions it is not so for the meteorological fields which induce variability from minutes to years in the chemical fields. Therefore, annual averages of the differences have also been calculated. As can be seen in figures 16 and 17 the seasonal differences persist also in the annual average.

To further consider the effect of noise statistical tests were conducted on monthly averaged fields. Considering the monthly time series in each grid point in the modelling domain we can pose the question whether the differences between the monthly averaged values in a grid point of the baseline and perturbed simulations are statistically significant and whether the differences between the monthly means are significant in a statistical sense. The tests were done for O_3, PM (which both contain the main secondary components) and SO_2 fields for July and January. In order to test if the variances of the time series being compared are similar a two-tailed F-test was performed under the null-hypothesis: the variance of the time series are identical; with the degrees of freedom being 743 (24 hours $\times$ 31 days -1) for all series. The F-values are shown in figure 18. Since all F-values are greater than 1 and less than than 1.19 (for these degrees of freedom the 99 % significance level corresponds to F = 1.19) we must accept the null hypothesis (to the 99 % significance level) and conclude that the variances are not significantly different. We then proceed and conduct a T-test for equal variances. Assuming equal variances the t-statistic for the null-hypothesis: the mean of the time series are identical may be seen in figure 19. Since the absolute value of the t-statistic exceeds the tabulated value of t at the 99 % significance level (2.329 at 743 $\times$ 743 degrees of freedom) for all species, we can reject the null hypothesis and conclude that the time series resulting from the baseline and perturbed simulations are significantly different to the 99 % level.

Final remarks and overview of results

Figure 20 gives an overview of the effect of insulation on regional air quality. They display the zone-averaged seasonal mean relative differences. The largest decreases

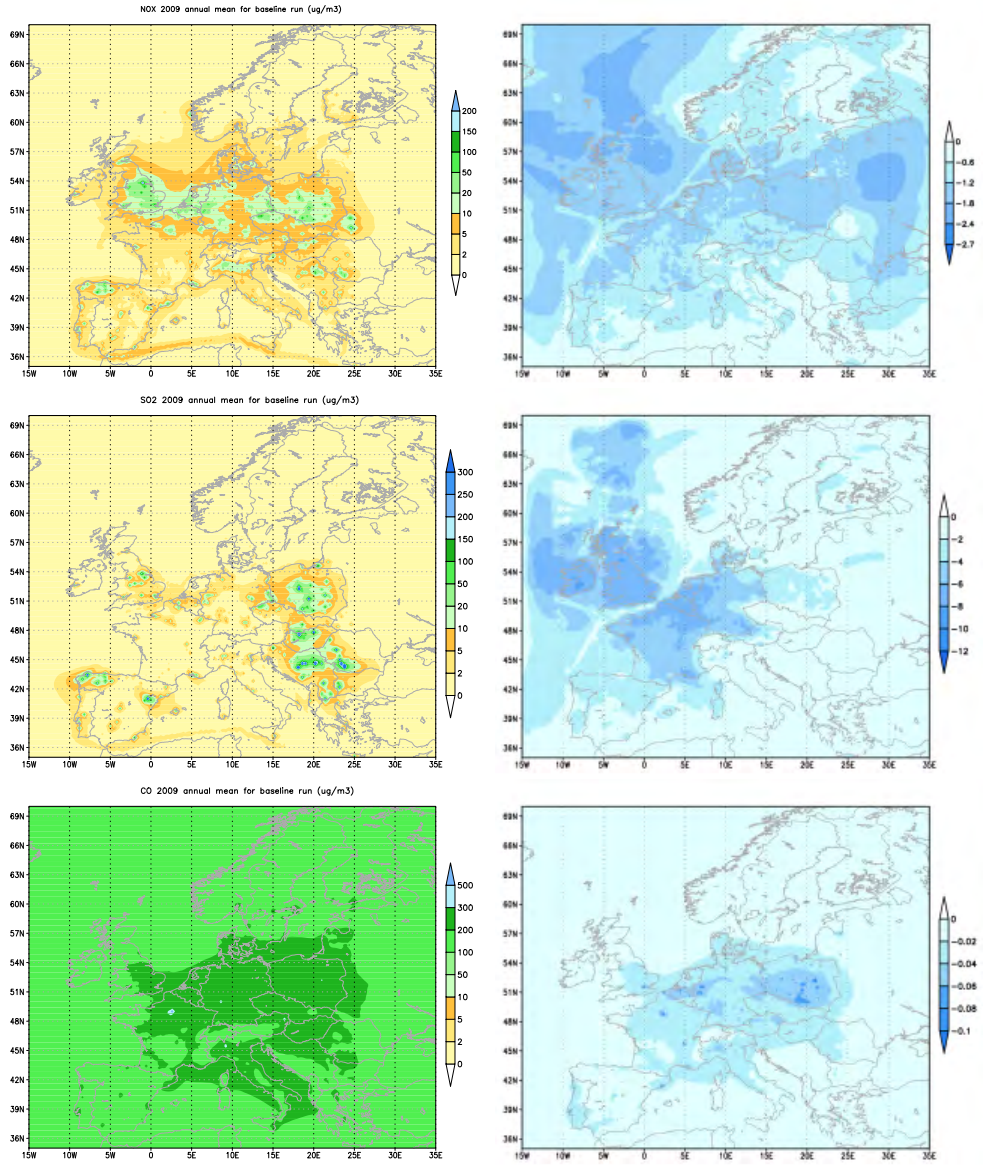

Figure 16: Annual averaged near-surface concentration ($\mu g\,m^{-3}$) of NO_x, SO_2 and CO (left column top to bottom) for the baseline scenario along with relative differences to the emission reduction scenario (right column).

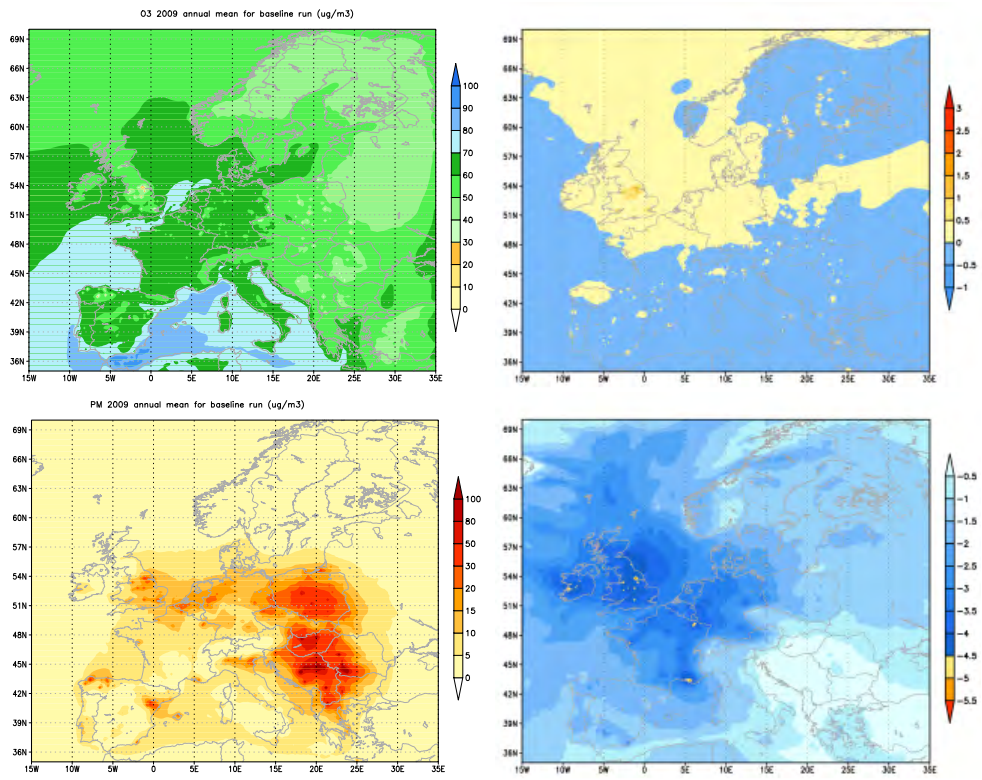

Figure 17: Annual averaged near-surface concentration ($\mu g\,m^{-3}$) of O_3 and PM (left column top to bottom) for the baseline scenario along with relative differences (%) to the emission reduction scenario (right column).

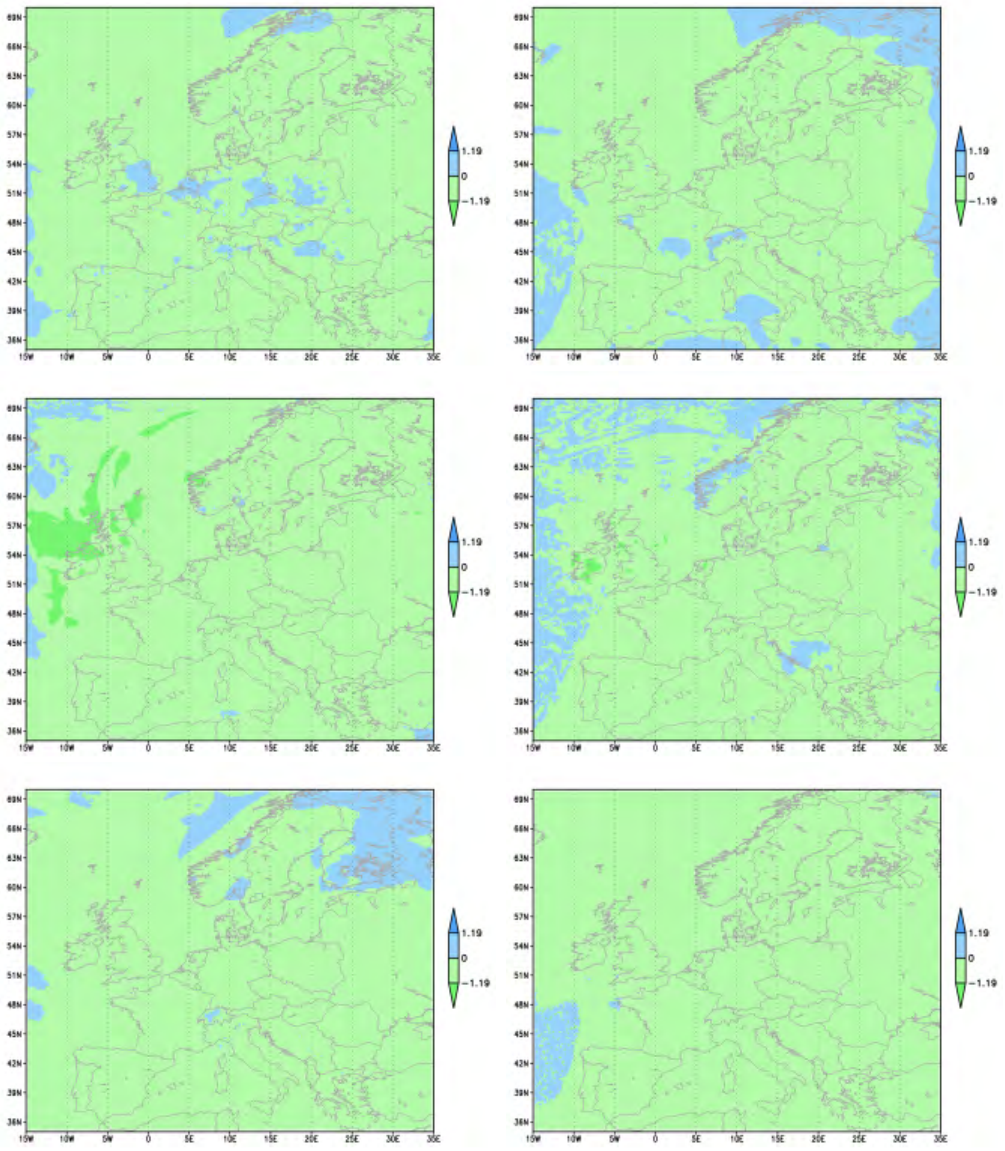

Figure 18: Values of the F-statistic calculated for O_3 (upper), SO_2 (middle) and PM (lower) for monthly time series of hourly values in January (left) and July (right).

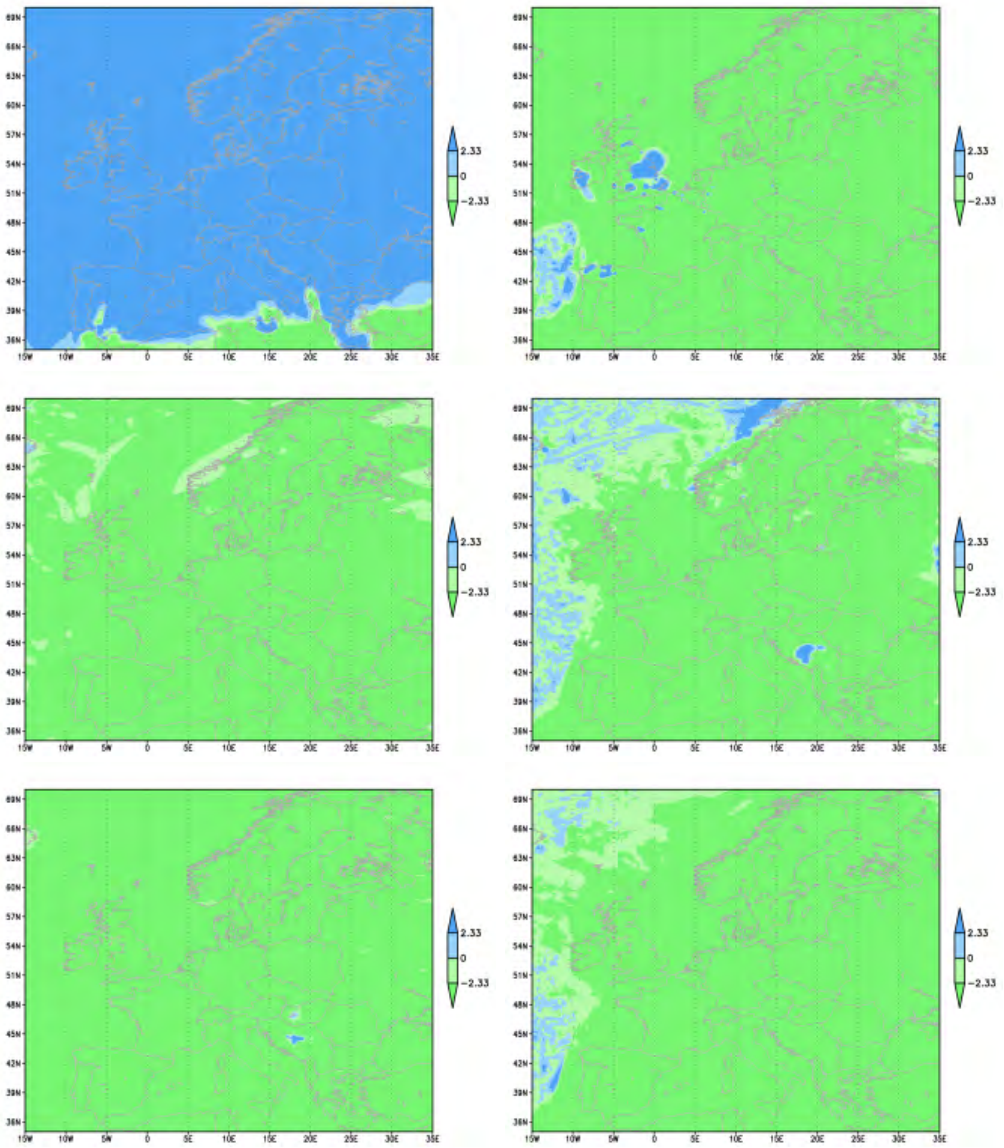

Figure 19: Values of the t-statistic calculated for O_3 (upper), SO_2 (middle) and PM (lower) for monthly time series of hourly values in January (left) and July (right).

are generally found in zone 2 for SO_2 and PM. Averaging over all seasons results in a decrease of 5.7 % for SO_2 and 3.1 % for PM. The largest NO_x decrease was found in zone 5 while some zones experienced increases in ozone concentrations outside the ozone season. These are connected to the increase found in mid-England, mainly during the winter season.

The purpose of this study was to estimate the effect of increased insulation levels on air pollutants on the regional scale. The emission reductions as calculated in section Emission estimation relies on the projected energy savings which are considered as regional averages over the EU member states. Therefore, the effect of energy and heat planning and policies in individual member states as well as their economical feasibility have not been considered here. Further issues that have not been incorporated in the present study include the influence of the initiation of a cap and trade program for NO_x and SO_2 in Europe and the effect of projected emission changes due to increased emission control strategies both on the political, industrial and technological level.

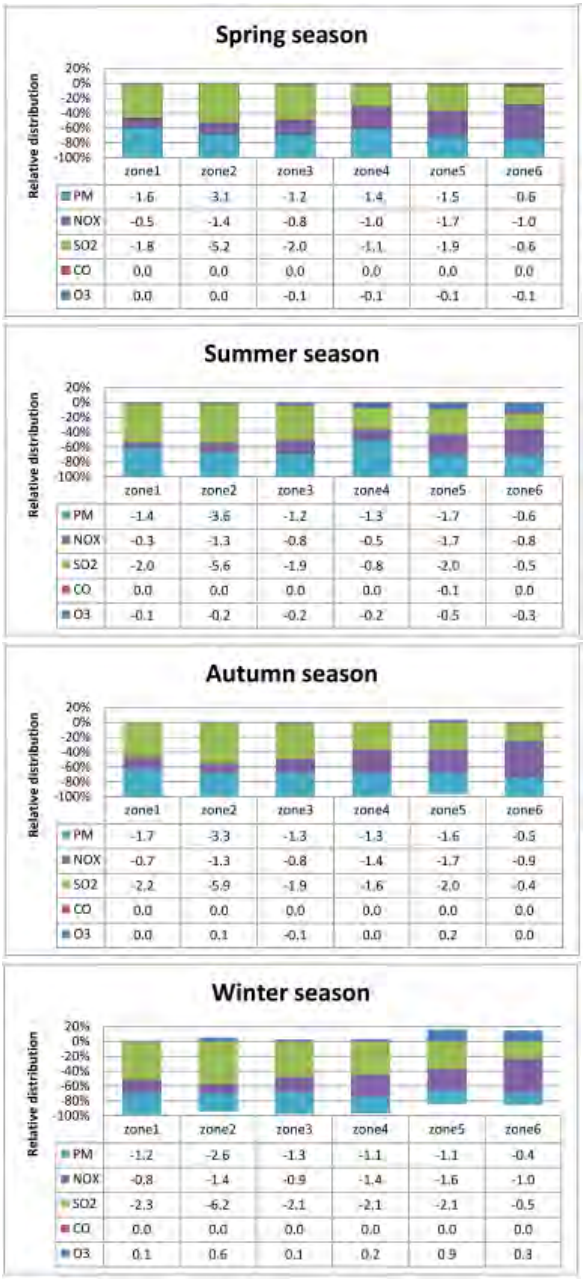

Figure 20: Zone averaged relative differences of NO_x, SO_2, CO, O_3 and PM for near-surface air (%). The bar chart shows the distribution of concentration changes within each zone.

Bibliography

Carter, W. P. L., 1996. Condensed atmospheric photooxidation mechanisms for isoprene. Atm. Env., 30, 4275-4290.

Chang, J. S., Brost, R. A., Isaksen, I. S. A., Madronich, S., Middleton, P., Stockwell, W. R., Walcek, C. J., 1987. A Three-dimensional Eulerian Acid Deposition Model: Physical Concepts and Formulation. J. Geophys. Res., 92, 14681-14700.

Colella, P., Woodward, P. R., 1984. The Piecewise Parabolic Method (PPM) for Gas-Dynamical Simulations. J. Comp. Phys., 54, 174-201.

ECOFYS, 2007. U-value for better energy performance of buildings.

ECOFYS, 2008. Impact assessment document for European Commission on a revised EPBD, Ecofys DG-TREN, 2008.

The Environ international coorporation, Comprehensive Air-Quality Model with Extensions version 5.20 (`http://www.camx.com`)

European Environment Agency, 2002. Electricity production by fuel, EU-25 (`http://www.eea.europa.eu/legal/copyright`) (`http://www.eea.europa.eu/data-and-maps/figures/electricity-production-by-fuel-eu-25`)

European Environment Agency, 2005. EN20 Combined Heat and Power (CHP) (`http://www.eea.europa.eu/legal/copyright`) (`http://www.eea.europa.eu/data-and-maps/indicators/en20-combined-heat-and-power-chp\#document-toc`)

European Environmental Agency, 2007. Latest Findings on National Air Quality - Status and Trends through 2006 (`http://www.epa.gov/air/airtrends/2007/`)

European Environment Agency, 2010. Air pollution by Ozone across Europe during summer 2009. Overview of exeedences of EC ozone threshold values for April-September 2009. technical report No. 2/2010, ISSN. 1725-2237, ISBN. 978-92-9213-090-9, doi. 10.2800/39256.

European Environment Agency, 2010. Global and European temperature (CSI 012) - Assessment, 2010 (`http://www.eea.europa.`

eu/data-and-maps/indicators/global-and-european-temperature/global-and-european-temperature-assessment-2)

Gery, M. W., Whitten, G. Z., Killus, J. P., Dodge, M. C., 1989. A photochemical kinetics mechanism for urban and regional scale computer modeling. J. Geophys. Res. ,94, 12925–12956.

Hertel, O., Berkowicz, R., Christensen, J., Hov, Ø., 1993. Test of two numerical schemes for use in atmospheric transport-chemistry models. Atm. Env., 27A, 2591-2611.

Jensen, O. M., Wittchen, K. B., Thomsen, K. E., EuroACE, 2009. Towards very low energy buildings. Energy saving and CO_2 reduction by changing European building regulations to very low energy standards. Statens Byggeforskningsinstitut, Aalborg University, report: SBi 2009:03. ISBN. 978-87-563-1361-2.

Korsholm, U. S., Baklanov, A., Gross, A., Sørensen J. H., 2009. On the importance of the meteorological coupling interval in dispersion modeling during ETEX-1. Atm. Env., doi:10.1016/j.atmosenv.2008.11.017.

Kuenen J., H. Denier van der Gon, A. Visschedijk, H. van der Brugh, S. Finardi, P. Radice, A. d'Allura, S. Beevers, J. Theloke, M. Uz-basich, C. Honorè, O. Perrussel (2010): A Base Year (2005) MEGAPOLI European Gridded Emission Inventory (Final Version). Deliverable D1.6, MEGAPOLI Scientific Report 10-17, MEGAPOLI-20-REP-2010-10, 39p, ISBN: 978-87-993898-8-9 (http://megapoli.dmi.dk/publ/MEGAPOLI_sr10-17.pdf)

Mosca, S., Bianconi, R., Bellasio, R., Graziani, G., Klug, W., 1998. European Tracer Experiment, ATMES II - Evaluation of long-range dispersion models using data of the 1st ETEX release. EUR17756EN. Office for official publications of the European Communities, Luxembourg. ISBN 92-828-3657X.

National Oceanic and Atmospheric Administration, National Climatic Data Center, 2009. State of the Climate, Global Analysis, Annual 2009 (http://www.ncdc.noaa.gov/sotc/global/2005/13).

Nenes, A. C., Pilinis, C., Pandis, S. N., 1998. ISORROPIA: A New Thermodynamic Model for Multiphase Multicomponent Inorganic Aerosols. Aquatic Geochemistry, 4, 123-152.

Reis, Júlio, 2004. Original author: http://commons.wikimedia.org/wiki/User\:Tintazul, (derived from original by: http://commons.wikimedia.org/wiki/User\:Kolja21) and is available from http://commons.wikimedia.org/wiki/File:\EU25-2004_European_Union_map_\enlargement.svg under the Creative Commons Attribution-Share Alike 2.5 Generic (CC-SA) license (http://creativecommons.org/licenses/by-sa/2.5/deed.en).

Strader, R., Lurmann, F., Pandis, S. S., 1999. Evaluation of secondary organic aerosol formation in winter. Atm. Env., 33, 4849-4863.

U. S. Environmental Protection Agency, AP 42, Fifth Edition, Compilation of Air Pollutant Emission Factors, Volume 1: Stationary Point and Area Sources with updates to 2009 (`http://www.epa.gov/ttn/chief/ap42/index.html`)

Wang, M. Q. Technical Report: GREET 1.5 – Transportation Fuel-Cycle Model - Volume 2: Appendixes of Data and Results, August, 1999. U.S department of Energy, Argonne national laboratory (`http://greet.es.anl.gov/publication-w1hsudgs`)

WMO World Data Centre for Greenhouse Gases and Japan Meteorological Agency: `http://gaw.kishou.go.jp/wdcgg/`. Courtesy the Federal Environment Agency (Umweltbundesamt), Air Monitoring Network, Germany, the Latvian Environment, Geology and Meteorology Centre, LVGMC, the Hungarian Meteorological Service and the Swedish Environmental Research Institute (IVL).

Yang, X., Kmit M., Pedersen, C., Nielsen, N. W., Sass, B. H., Amstrup, B., 2005. The DMI-HIRLAM upgrade in November 2005. DMI Technical Report 05-15, `http://www.dmi.dk/dmi/tr05-15.pdf`.

Yang, X., Kmit M., Sass, B. H., Amstrup, B., Lindberg, K., Pedersen, C., Korsholm, U. S., Nielsen, N. W., 2005. The DMI-HIRLAM upgrade in May 2005. DMI Technical Report 05-10, `http://www.dmi.dk/dmi/tr05-10.pdf`.